Assessing the role of human mobility on malaria transmission

Abdulaziz Y.A. Mukhtar[1,2*], Justin B. Munyakazi[1], and Rachid Ouifki[3]

[1]Department of Mathematics and Applied Mathematics, University of the Western Cape, Private Bag X17, Bellville 7535, South Africa
[2]DST-NRF Centre of Excellence in Mathematical and Statistical Sciences (CoE-Mass)
[3] Department of Mathematics and Applied Mathematics, Faculty of Natural & Agricultural Sciences, University of Pretoria, Private Bag X20, Hatfield 0028, South Africa

December 30, 2019

Abstract

South Sudan accounts for a large proportion of all annual malaria cases in Africa. In recent years, the country has witnessed an unprecedented number of people on the move, refugees, internally displaced people, people who have returned to their countries or areas of origin, stateless people and other populations of concern, posing challenges to malaria control. Thus, one can claim that human mobility is one of the contributing factors to the resurgence of malaria. The aim of this paper is to assess the impact of human mobility on the burden of malaria disease in South Sudan. For this, we formulate an SIR-type model that describes the transmission dynamics of malaria disease between multiple patches. The proposed model is a system of stochastic differential equations consisting of ordinary differential equations perturbed by a stochastic Wiener process. For the deterministic part of the model, we calculate the basic reproduction number. Concerning the whole stochastic model, we use the maximum likelihood approach to fit the model to weekly malaria data of 2011 from Central Equatoria State, Western Bahr El Ghazal State and Warrap State. Using the parameters estimated on the fitted model, we simulate the future observation of the disease pattern. The disease was found to persist in the low transmission patches when there is human inflow in these patches and although the intervention coverage reaches 75%.

Keywords: Malaria, Movement, Stochastic model, Maximum likelihood, Basic reproduction number.

[0]*Corresponding author. E-mail: amukhtar@uwc.ac.za.

1 Introduction

Malaria is a vector-borne disease that causes a lot of distress to people on a global scale. In spite of recent achievements in the fight against malaria, which has led to a significant reduction in the burden, the disease still counts amongst the top ten deadly diseases in the world with an estimate of 400 000 deaths each year [42].

Malaria is transmitted more robustly and incessantly in Africa than it is elsewhere. Further constraints regarding malaria dynamics complexity, are the recurring outbreaks of conflicts on the continent which contribute to a large number of people's displacement and migration, increasing their vulnerability to infectious diseases [15, 19].

In this paper we focus mainly on South Sudan, the youngest country in Africa which has just emerged from two decades of civil war and sporadic violence. This has steered to a deteriorating socioeconomic situation, collapsed health systems and disruption of disease control programs. For instance, in the rural areas, the disease exerts an enormous toll due to poor health services and lack of sufficient transport whereby people travel long hours to reach the nearest health facility. The political unrest has further led to substantial population mobility including mass population displacements [15]. There are an estimated 1.61 million Internally Displaced People (IDPs), and over 975,801 refugees in neighboring countries [34]. It was reported that in 2013 almost all states were affected directly or indirectly by conflict-induced displacement, as shown in Figure 1. The fluidity of displacement in the country makes it difficult for health care providers to reach all conflict-affected populations. Moreover, the displaced people are associated with poor-quality housing that makes them more vulnerable to mosquito bites and thus increases the risk factor for malaria. If displaced people are not immunized, they may move to malarious regions and acquire the infection, and if they are infectious, they may disseminate the infection to other areas. Consequently, vector-borne diseases in particular malaria, across many areas of the country have worsened. With this backdrop, it is more difficult to comprehend how the epidemic is circulating among the population.

Mathematical models for malaria transmission can help better understand the occurrence of the disease in the community and investigate how certain factors such as migrations affect the course of the epidemic. In this regards, several mathematical models have been developed by researchers starting from the basic malaria model of Ross [37] and Macdonald [23] to more complex models considering different factors relating to malaria transmission dynamics and control [12, 13, 18, 3, 10, 26, 19, 24, 29, 33, 41].

In a review article, Cosner et al.[9] explored optimal disease control in spatial environment using models that account human mobility between patches. In a recent study, Cosner et al. [8] showed, using empirical data combined with mathematical analyses, a significant effect of host and vector movement patterns on the disease burden. Kim et al. [21] pointed up the importance of border screening in the presence of human migration in Africa during an outbreak. Acevedo et al.[1] explored analytically and via numerical simulations how human mobility and spatial variation in transmission influence malaria long-term persistence determined by the basic reproduction number R_0, and prevalence. They show that movement can reduce heterogeneity in exposure to mosquito biting. When local transmission rates are highly heterogeneous, R_0 declines

asymptotically as human mobility increases.

Using a two-patch model, Gao and Ruan [14] demonstrated that human movement can aid malaria to turn from disease-free to endemic equilibria in both patches, even though malaria could be eradicated in each patch when isolated. Their study points out that R_0 varies monotonously with the movement of exposed, infectious and recovered humans and hence human movement is a critical factor in the spatial spread of malaria around the world.

Malaria occurrence may be accentuated critically by factors such as environmental change, socioeconomic situation, and human mobility. For this reason, improving our perception of host-parasite interactions that attests to the seriousness of these factors is crucial. In our previous study [27], we focused on understanding the significant role that temperature and rainfall play in the dynamics of the mosquito populations in the study of malaria transmission in South Sudan. More precisely the study helps understand the course of malaria epidemic in two different climatic regions experiencing climate change, also gain insight into the abundance of mosquitoes with changes in rainfall and temperature patterns within the region that alter the volatility of malaria cases throughout the year. Consequently, the study proposed and analyzed a human-mosquito disease-based model that includes temperature and rainfall on the mosquito component. The results reflect that disease is more effective and severe in the tropical region than in a hot semi-arid region of South Sudan. Note this study focused more on mosquito population and how this is impacted by climate factor. This explain why

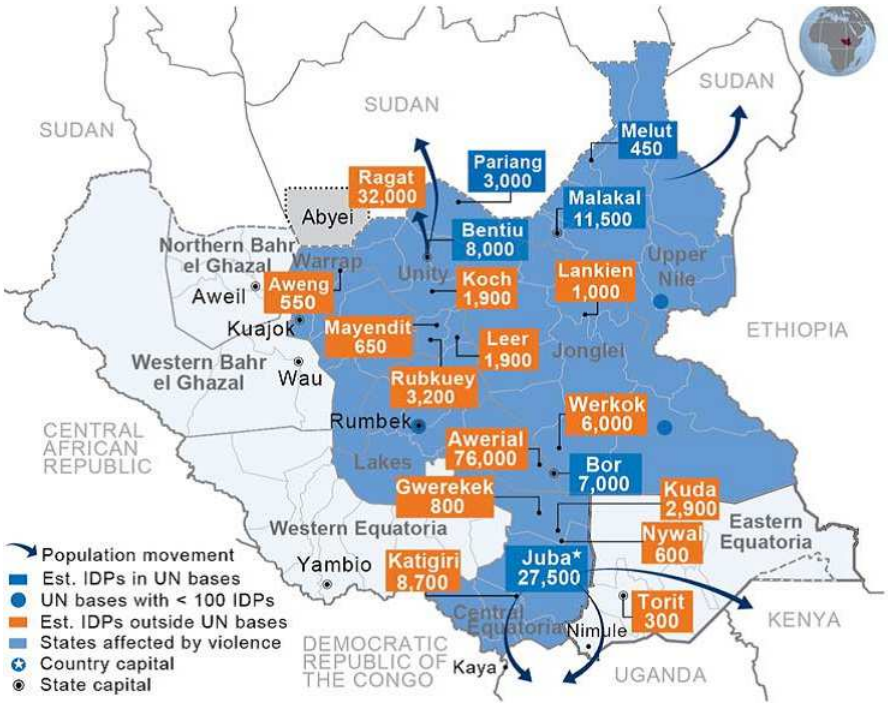

Figure 1: Source: [34], IDPs camp and movement patterns

asymptomatic infection class for human was not included in the study.

In a different study [28], the focus of the study shifted to humans where intervention variables were incorporated to contract the spread of malaria. Thus we added the asymptomatic malarial infections compartment in this case. In both of the above-mentioned works, human mobility is not taken into consideration in the transmission of malaria. Hence, this study seeks to assess whether human mobility may have an impact on the malaria epidemic in South Sudan. The model generalizes the mosquito biting rate for each patch so that it applies to wider ranges of populations. We consider that the total number of mosquito bites on humans depends only on the number of mosquitoes, similar to that model of [28, 30].

The deterministic modeling based on ordinary differential equations (ODEs) is the most widely used approach. The inclusion of stochasticity in a mathematical model may be motivated by demographic fluctuations resulting from the stochastic nature of the epidemic, randomization in the environment or observed stochasticity that include diagnostic errors, incomplete reporting of cases or fluctuations of the reporting rate. These sources have the ability to make stochastic model behaviour quite different from that of a deterministic performance, such as in [20, 22, 25, 43, 40] for example.

In this study, we thought to include stochastic scenarios to the model due to the important properties such as the probability of an outbreak, final size distribution of an epidemic and the expected duration of an epidemic that depends on the stochastic nature of the process related to the randomness scenarios of human mobility.

There are three types of stochastic processes namely the discrete-time Markov chain (DTMC) model, a continuous-time Markov chain (CTMC) model and a stochastic differential equation (SDE) model where their simulation results are similar in a short time [2]. We consider SDE processes to be formulated for the well-known SEIAR epidemic model where its sample paths remain continuous.

The fact that most of the stochastic systems run scenarios several thousand times stochastically can better explain the variability of the observed time-series. This process provides a way of interpreting results using confidence bands.

The present study considers demographic stochasticity based on the variability of the epidemical process by using a stochastic model based on a diffusion process, so as to minimize uncertainty in the modeling process to give realistic measures of confidence around predictions with reliable population projections. To accommodate such stochasticity, we extend a classical deterministic SIR-type epidemic model with migration flows by adding a stochastic noise term in the form of a Wiener process to the human component of our basic model 2.1. This strategy makes sense because the mobility of mosquito is negligible as compared to the distance between study patches. To estimate the model's parameter we use maximum likelihood to fit it to weekly malaria data of 2011 from Central Equatoria State, Western Bahr El Ghazal State and Warrap State.

2 Model formulation

In this section, we begin with the formulation of a deterministic metapopulation malaria epidemic model which we further extend by adding a white noise perturbation. The deterministic part of the model is based on the SEIAR-SEI model of [28], in which we incorporate human migration factors similar to that considered [21]. The human components in the model are utilized to capture disease dynamics and population's movement. Conflicts force individual irrespective of their health status to flee to safer zones. For the purpose of our study, the migration factors considered in our model formulation account for movement of people between n different regions. We assume that disease transmission conditions are homogeneous within each of these regions. Subsequently, we divide the human population in each patch i, N_i (with $i = 1, \ldots, n$) into susceptible individuals S_i, pre-infectious individuals with malaria parasite E_i, individuals with malaria symptoms I_i, asymptomatic infectious individuals A_i and recovered individuals R_i, so that

$$N_i(t) = S_i(t) + E_i(t) + I_i(t) + A_i(t) + R_i(t).$$

Accordingly, we assume that individuals of all disease classes are subject to migration flows between patches. Although some individuals, during their travel, may change their disease status (for instance from susceptible to latently infected or symptomatic disease), we assume, for simplicity, that individuals keep their disease status as they move between patches. Subsequently, for each disease state $Q = S, E, I, A, R$, individuals are assumed to immigrate from patch j to patch i at rate $\psi_{i,j}^{Q}$ without changing their states. The disease transmission dynamics and population's migration are considered to have both deterministic and stochastic components that operate simultaneously. This provides an additional degree of realism compared to deterministic models. In order to account for stochasticity, we introduce white noise stochastic perturbations onto deterministic model, and formulate the necessary assumptions *hitherto*. Additionally, the mosquito components in the model are represented to capture the effects of vector control in preventing transmission. We consider Anopheles *Gambiae* mosquitoes which are the main anopheles species that transmit *Plasmodium Falciparum* in South Sudan. The total mosquito population M_i is divided into susceptible mosquitoes X_i, mosquitoes exposed to the malaria parasite Y_i, and infectious mosquitoes Z_i, that is

$$M_i(t) = X_i(t) + Y_i(t) + Z_i(t).$$

The population dynamics and infection processes of human and anopheles *Gambiae* mosquitoes are given by the following set of ordinary differential equations:

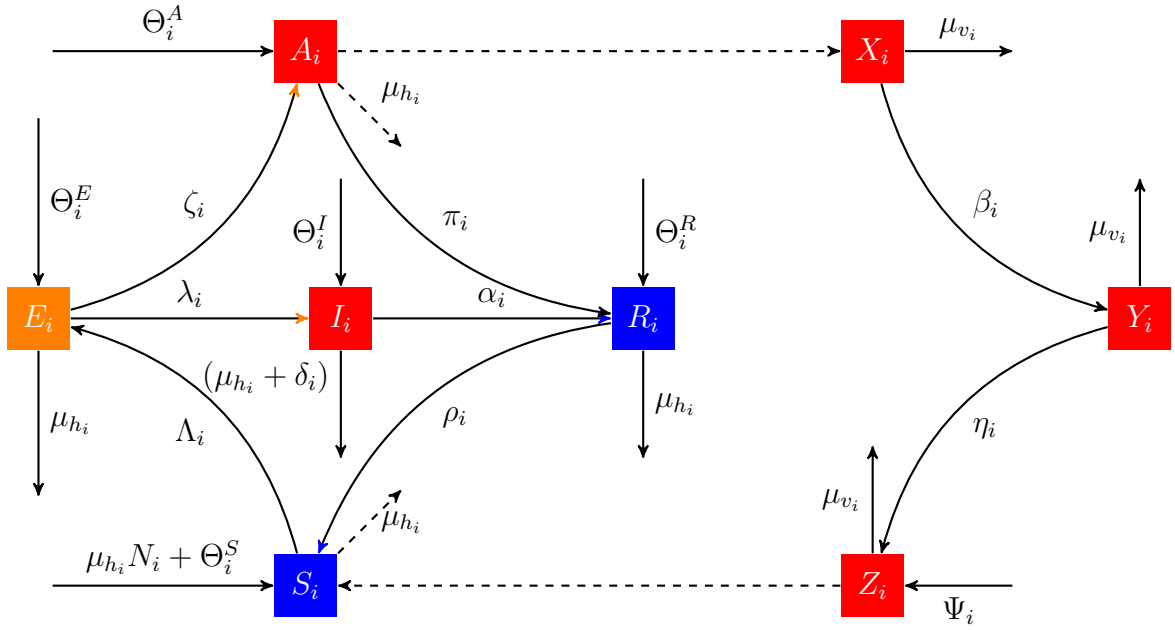

Figure 2: Model flow diagram for human and mosquito populations in State i, where $\Theta_i^Q = \sum_{j\neq i=1}^{n} \psi_{j,i}^Q Q_j - \sum_{j\neq i=1}^{n} \psi_{i,j}^Q Q_i$, with $Q \in \{S, E, I, A, R\}$.

$$
\left.
\begin{aligned}
\tfrac{dS_i}{dt} &= \Gamma_i - \Lambda_i S_i - \mu_{h_i} S_i + \rho_i R_i + \textstyle\sum_{j\neq i=1}^{n} \psi_{j,i}^S S_j - \sum_{j\neq i=1}^{n} \psi_{i,j}^S S_i \\
\tfrac{dE_i}{dt} &= \Lambda_i S_i - (\lambda_i + \zeta_i + \mu_{h_i}) E_i + \textstyle\sum_{j\neq i=1}^{n} \psi_{j,i}^E E_j - \sum_{j\neq i=1}^{n} \psi_{i,j}^E E_i \\
\tfrac{dI_i}{dt} &= \lambda_i E_i - (\alpha_i + \delta_i + \mu_{h_i}) I_i + \textstyle\sum_{j\neq i=1}^{n} \psi_{j,i}^I I_j - \sum_{j\neq i=1}^{n} \psi_{i,j}^I I_i \\
\tfrac{dA_i}{dt} &= \zeta_i E_i - (\pi_i + \mu_{h_i}) A_i + \textstyle\sum_{j\neq i=1}^{n} \psi_{j,i}^A A_j - \sum_{j\neq i=1}^{n} \psi_{i,j}^A A_i \\
\tfrac{dR_i}{dt} &= \alpha_i I_i + \pi_i A_i - (\rho_i + \mu_{h_i}) R_i + \textstyle\sum_{j\neq i=1}^{n} \psi_{j,i}^R R_j - \sum_{j\neq i=1}^{n} \psi_{i,j}^R R_i \\
\tfrac{dX_i}{dt} &= \Psi_i - \beta_i X_i - \mu_{v_i} X_i dt \\
\tfrac{dY_i}{dt} &= \beta_i X_i - (\eta_i + \mu_{v_i}) Y_i \\
\tfrac{dZ_i}{dt} &= \eta_i Y_i - \mu_{v_i} Z_i
\end{aligned}
\right\}. \tag{2.1}
$$

where $S_i > 0$, $E_i \geq 0$, $I_i \geq 0$, $A_i \geq 0$, $R_i \geq 0$, $X_i \geq 0$, $Y_i \geq 0$, $Z_i \geq 0$, the terms Λ_i and β_i are the forces of infection that we follow the approach in [30, 27] to model:

- $\Lambda_i(Z_i, N_i) = \dfrac{\epsilon_i b_i Z_i}{N_i}$, represents the force of infection on humans defined as the

product of;
$\epsilon_i S_h M_i/N_i$, the average number of bites given to susceptible humans by each mosquito per unit time to be measured at study settings level i;
b_i, the probability of an infected mosquito bite causes infection in a susceptible human;
Z_i/M_i, the proportion of the total number of bites that are potentially infectious to humans.

- $\beta_i(A_i, I_i, N_i) = \dfrac{\epsilon_i(\kappa_i A_i + \nu_i I_i)}{N_i}$, represents the force of infection on mosquitoes which is defined similarly as on humans, assuming that the reservoir of possible infections from humans includes ν_i and κ_i defined as the probability that a susceptible mosquitoes bite on an infected human to transfer the infection to the mosquito from a clinical infectious and an asymptomatic infectious human respectively, excluding a recovery stage to be releasing merozoites into the bloodstream.

Table 1: Model Variables

S_i	Susceptible individuals
E_i	Pre-infectious individuals with malaria parasite
I_i	Individuals with malaria symptoms
A_i	Asymptomatic infectious individuals
R_i	Recoved individuals
X_i	Susceptible mosquitoes
Y_i	Mosquitoes exposed to the malaria parasite
Z_i	Infectious mosquitoes

The susceptible individuals is recruited by birth at a rate $\Gamma_i = \mu \times N_i$ where N_i is the total human population size for patch i. We assume that transmission occurs solely between humans and mosquiotes from the same state; subsquently susceptible human (S_i) in patch i acquire malaria and become pre-infectious and move to class E_i at a rate Λ_i when they are bitten by infectious mosquitoes from the same patch i. Thereafter, according to the clinical studies [11, 18], individuals either develop clinical infection and progress to the infectious compartment I_i at the rate λ_i (that is the inverse of the duration of the latent period of 12 days on average) or progress to the asymptomatic class A_i at the rate ζ_i after an average period of 20 days. In this study, the parameters ζ and λ are estimated during the data fitting process for each patch using the durations above as prior knowledge. Those that develop disease are successfully treated at rate α_i and subsequently enter a period of prophylaxis (recovery compartment R_i). The disease-induced mortality rate is denoted by δ_i. Individuals with asymptomatic infection are assumed to recover naturally with a constant per capita recovery rate π_i and enter R_i compartment. Depending on the type of treatment that may be used to recover from infection, individuals from recovery class move to the

susceptible compartment at rate ρ_i when they lose their temporary immunity. This is validated with data from a long-term trial in [18, 31].

Some studies have indicated that super-infection (that is infectious individuals being inoculated with more parasite in addition to the original infection) is possible to occur in both clinical and asymptomatic classes [7, 18, 31]. However, since other studies have shown that the occurrence of super-infection can be regarded as a rare event [31, 32], we chose to ignore it in this model.

All compartments are stratified in patch i by a level where individuals are bitten by mosquitoes and population are declining with a natural mortality rate of $\mu_{h_i} = \frac{1}{q \times 360} day^{-1}$ where q is the human life expectancy in years. Susceptible female mosquitoes in patch i are recruited at the birth rate Ψ_i. We assume that reduction in the susceptible mosquitoes occurs through natural death at rate μ_{v_i}, or through infection at rate β_i. At this rate β_i susceptible mosquitoes move to the pre-infectious class Y_i (pass through a latent period of fixed length) from the same patch i. Latently

Table 2: Model parameters

Symbols	Description
Γ	Per ca-pita birth rate of Humans. Humans/Day^{-1}
ψ	Immigration rate of humans. Day^{-1}
μ_h	Natural mortality rate of humans. Day^{-1}
δ	Mortality rate of humans due to malaria. Day^{-1}
ϵ	The average number of bites given to humans by each mosquito per unit time.
b	Probability of transmitting malaria to susceptible humans from an infectious mosquito provided that contact occurs between the two.
ν	Probability of transmitting malaria to susceptible mosquitoes from a clinical infectious human-provided that contact occurs between the two.
κ	Probability of transmitting malaria to susceptible mosquitoes from an asymptomatic infectious human-provided that contact occurs between the two.
λ	Progression rate of humans from pre-infectious state to a clinical infectious state, that is the reciprocal of the duration of the latent period. Day^{-1}
ζ	Progression rate of humans from pre-infectious state to asymptomatic infectious state, that is the reciprocal of the duration of the patent infection. Day^{-1}
α	Per ca-pita recovery rate for humans from clinical infectious state to the recovered state, that is the reciprocal duration of the infectious period. Day^{-1}
π	Per ca-pita recovery rate for humans from asymptomatic infectious state to the recovered state, that is the reciprocal duration of the sub-patent infection period. Day^{-1}
ρ_i	Per ca-pita rate of loss of immunity, that is the reciprocal duration of the immune (Prophylaxis following treatment) period. Day^{-1}
η	Progression rate of mosquitoes from pre-infectious state to infectious state.
μ_v	Daily mosquito mortality.
Ψ	Per ca-pita birth rate of mosquitoes.

infected mosquitoes move at rate η_i to infectious mosquitoes class and remain in that class until they die at rate μ_{v_i}. We note here that we made all mosquito parameters depend on the patch they live in to reflect dependency on some internal factors such as temperature and rainfall.

The population dynamics for these patches is considered to have both deterministic and stochastic components that operate simultaneously. Of course, the dynamics of stochastic models for an epidemic population provide an additional degree of realism compared to their deterministic counterparts. Fluctuations in demographic stochasticity conditions are some of the most important factors affecting real world systems. A large part of natural phenomena do not follow deterministic laws exactly, but rather oscillate randomly around some average values [20, 25]. We introduce white noise stochastic perturbations on the deterministic model equations of human component and we formulate the necessary assumptions hitherto. We assume that movements of individuals in and out of a particular patch are independent and fluctuations in population size due to random demographic events do not necessarily lead to extinction.

We ignore randomness in mosquito equations since we excluded in this study the environmental (external) factors that act on the epidemiological processes. Hence, the resulting model consists of a system of stochastic differential equations (SDEs) comprising of deterministic terms which are perturbed by a white noise. Therefore, in this paper we propose to examine the effects of the introduction of demographic stochasticity noise on the positivity and boundedness of the stochastic process solution of the mathematical model proposed in 2.1.

Model (2.1) based on our previous work of [28] has the disease-free equilibrium

$$E_0 = (S^*, E^*, I^*, A^*, R^*, X^*, Y^*, Z^*) = (\frac{\Gamma}{\mu}, 0, 0, 0, 0, \frac{\Psi}{\mu_v}, 0, 0)$$

and an endemic equilibrium if $\mathcal{R}_0 > 1$. The disease-free equilibrium is globally asymptotically stable if $\mathcal{R}_0 < 1$ and unstable if $\mathcal{R}_0 > 1$. These results of model (2.1) were studied when $\Theta_i^Q = 0$ where $Q \in \{S, E, I, A, R\}$. If we add $\Theta_i^Q + \sigma_Q(dW_Q/dt)$ on human component of the model, where (dW_Q/dt) is a white noise (i.e., W(t) is a Brownian motion), model (2.1) becomes

$$\begin{cases} dS_i = \left[\Gamma_i - \Lambda_i S_i - \mu_{h_i} S_i + \rho_i R_i + \sum_{j\neq i=1}^{n} \psi_{j,i}^{S} S_j - \sum_{j\neq i=1}^{n} \psi_{i,j}^{S} S_i\right] dt + \sigma_S S_i dW_S(t) \\ dE_i = \left[\Lambda_i S_i - (\lambda_i + \zeta_i + \mu_{h_i}) E_i + \sum_{j\neq i=1}^{n} \psi_{j,i}^{E} E_j - \sum_{j\neq i=1}^{n} \psi_{i,j}^{E} E_i\right] dt + \sigma_E E_i dW_E(t) \\ dI_i = \left[\lambda_i E_i - (\alpha_i + \delta_i + \mu_{h_i}) I_i + \sum_{j\neq i=1}^{n} \psi_{j,i}^{I} I_j - \sum_{j\neq i=1}^{n} \psi_{i,j}^{I} I_i\right] dt + \sigma_I I_i dW_I(t) \\ dA_i = \left[\zeta_i E_i - (\pi_i + \mu_{h_i}) A_i + \sum_{j\neq i=1}^{n} \psi_{j,i}^{A} A_j - \sum_{j\neq i=1}^{n} \psi_{i,j}^{A} A_i\right] dt + \sigma_A A_i dW_A(t) \\ dR_i = \left[\alpha_i I_i + \pi_i A_i - (\rho_i + \mu_{h_i}) R_i + \sum_{j\neq i=1}^{n} \psi_{j,i}^{R} R_j - \sum_{j\neq i=1}^{n} \psi_{i,j}^{R} R_i\right] dt + \sigma_R R_i dW_R(t) \\ dX_i = \left[\Psi_i - \beta_i X_i - \mu_{v_i} X_i\right] dt \\ dY_i = \left[\beta_i X_i - (\eta_i + \mu_{v_i}) Y_i\right] dt \\ dZ_i = \left[\eta_i Y_i - \mu_{v_i} Z_i\right] dt \end{cases} \tag{2.2}$$

Since it is a population system, it is important that we do not obtain negative values. In order to find conditions of existence of unique positive global solution of the stochastic epidemic model, we use the method of Lyapunov functions. Let $(\Omega, \mathcal{F}, \{\mathcal{F}_t\}_{t\geq t_0}, P)$ be a probability space which is right continuous with a filtration $\{\mathcal{F}_t\}_{t\geq t_0}$. Let $C^{2,1}(\mathbb{R}^5 \times [0,\infty); \mathbb{R}_+)$ be the family of all nonnegative functions $V(x,t)$ defined on $\mathbb{R}^5 \times [0,\infty)$ which are continuously twice differentiable in x and once in t. Let $W(t) = (W_S(t), W_E(t), W_I(t), W_A(t), W_R(t))$ a 5-dimensional Wiener process defined on this probability space. The non-negative constants σ_S, σ_E, σ_I, σ_A and σ_R denote the intensities of the stochastic perturbations. We shall assume that the components of the 1-dimensional Wiener process W_i are mutually independent. It is important to show that the SDE model (2.2) has at least a unique global solution in order for the model to have meaning and also that the solution will remain positive whenever the initial conditions are positive. Thus, the following theorem:

Theorem 1. *For model (2.2) and any initial value in $\mathbb{R}_+^{8n}$, there is a unique solution $L = (S_i(t), E_i(t), I_i(t), A_i(t), R_i(t), X_i(t), Y_i(t), Z_i(t))_{i=1,\cdots,n}$, of the system (2.2) for $t \geq 0$ which will remains in $\mathbb{R}_+^{8n}$ with probability one.*

Proof. The total human population in system (2.2) verifies the equation (2.3) with the initial value $\mathrm{N}_i(0) = S_i(0) + E_i(0) + I_i(0) + A_i(0) + R_i(0)$,
if $(S_i(s), E_i(s), I_i(s), A_i(s), R_i(s),)_{i=1,\cdots,n} \in \mathrm{R}_+^{5n}$ for all $0 \leq s \leq t$ almost surely (a.s)

$$dN_i(t) < [\mathbf{\Gamma}_i - \varphi N_i] \text{ a.s} \tag{2.3}$$

where

$$\begin{cases} \mathbf{\Gamma}_i = \sum_{j\neq i=1}^{n} \psi_{i,j}^{Q} N_j + \Gamma_i \text{ for } Q = S, R \text{ and } j = 1, \cdots, n, \ j \neq i \\ \varphi = \mu_{h_i} + \sum_{j\neq i=1}^{n} \psi_{i,j}^{Q}. \end{cases}$$

Hence, by integration we check

$$N_i(s) < \frac{\mathbf{\Gamma}_i}{\varphi} + (N_i(0) - \frac{\mathbf{\Gamma}_i}{\varphi}) \exp(-\varphi s) \text{ for all } s \in [0,t] \text{ a.s .}$$

Then

$$N_i(s) < \frac{\mathbf{\Gamma}_i}{\varphi} \text{ if assumed } N_i(0) < \frac{\mathbf{\Gamma}_i}{\varphi} \text{ so}$$

$$(S_i(s), E_i(s), I_i(s), A_i(s), R_i(s),)_{i=1,\cdots,n} \in (0, \frac{\mathbf{\Gamma}_i}{\varphi}) \text{ for all } s \in [0,t] \text{ a.s .} \tag{2.4}$$

Note that the coefficients of the system (2.2) are locally Lipschitz continuous, for any given initial value, there is a unique maximal local solution $(S_i(t), E_i(t), I_i(t), A_i(t), R_i(t), X_i(t), Y_i(t), Z_i(t))_{i=1,\cdots,n}$ on $t \in [0, \tau_e)$, where τ_e is the explosion time (see e.g., [4, 17]).

To show this solution is global, we need to show that $\tau_e = \infty$ almost surely (a.s). Let $m_0 > 0$ such that $(S_i(0), E_i(0), I_i(0), A_i(0), R_i(0), X_i(0), Y_i(0), Z_i(0))_{i=1,\cdots,n} \in [\frac{1}{m_0}, m_0]$. For each integer $m \geq m_0$, define a sequence of stopping times by

$$\tau_m = \inf \left\{ t \in [0, \tau_e) : S(t), E(t), I(t), A(t), R(t), X(t), Y(t) \text{ or } Z(t) \notin \left(\frac{1}{m}, m \right) \right\}$$

where we set $\inf \emptyset = \infty$. Now since τ_m is nondecreasing, the following limit exists: $\tau_\infty = \lim_{m \to \infty} \tau_m$, and $\tau_\infty \leq \tau_e$ (a.s.). We need to show that $\tau_\infty = \infty$ a.s.
If this statement is violated, then there exists $T > 0$ and $\epsilon \in (0,1)$ such that

$$\mathbb{P}\{\tau_\infty \leq T\} > \epsilon. \tag{2.5}$$

Thus, there is an integer $m_1 \geq m_0$ such that

$$\mathbb{P}\left\{\tau_m \leq T\right\} \geq \epsilon, \text{ for all } m \geq m_1.$$

Define a C^2-function $V : \mathbb{R}^{8n}_+ \to \mathbb{R}_+$ by

$$\begin{aligned} V(L) = \; & \textstyle\sum_{i=1}^n \Big[(S_i - 1 - \ln S_i) + (E_i - 1 - \ln E_i) + (I_i - 1 - \ln I_i) + (A_i - 1 - \ln A_i) \\ & + (R_i - 1 - \ln R_i) + (X_i - 1 - \ln X_i) + (Y_i - 1 - \ln Y_i) + (Z_i - 1 - \ln Z_i) \Big] \end{aligned}$$

By applying Itô's formula we get,

$$\begin{aligned} dV(L) = \; & \textstyle\sum_{i=1}^n \Big[\left(1 - \frac{1}{S_i}\right) dS_i + \frac{1}{2S_i^2} dS_i dS_i + \left(1 - \frac{1}{E_i}\right) dE_i + \frac{1}{2E_i^2} dE_i dE_i \\ & + \left(1 - \frac{1}{I_i}\right) dI_i + \frac{1}{2I_i^2} dI_i dI_i + \left(1 - \frac{1}{A_i}\right) dA_i + \frac{1}{2A_i^2} dA_i dA_i \\ & + \left(1 - \frac{1}{R_i}\right) dR_i + \frac{1}{2R_i^2} dR_i dR_i + \left(1 - \frac{1}{X_i}\right) dX_i + \frac{1}{2X_i^2} dX_i dX_i \\ & + \left(1 - \frac{1}{Y_i}\right) dY_i + \frac{1}{2Y_i^2} dY_i dY_i + \left(1 - \frac{1}{Z_i}\right) dZ_i + \frac{1}{2Z_i^2} dZ_i dZ_i, \Big] \end{aligned}$$

and using (2.2) we obtain

$$\begin{aligned} dV(L) = \; & \mathcal{L}V dt + \left(1 - \frac{1}{S_i}\right) \sigma_S S_i dW_S(t) + \left(1 - \frac{1}{E_i}\right) \sigma_E E_i dW_E(t) + \left(1 - \frac{1}{I_i}\right) \sigma_I I_i dW_I(t) \\ & + \left(1 - \frac{1}{A_i}\right) \sigma_A A_i dW_A(t) + \left(1 - \frac{1}{R_i}\right) \sigma_R R_i dW_R(t) \end{aligned}$$

where

$$\begin{aligned}\mathcal{L}V = \; & \textstyle\sum_{i=1}^{n} \frac{\epsilon_i b_i Z_i}{N_i} - \frac{\epsilon_i b_i S_i Z_i}{N_i E_i} + \mu_{h_i} N_i + \zeta_i + \lambda_i + \rho_i + \alpha_i + \delta_i + \pi_i \\ & + \textstyle\sum_{i=1}^{n} \frac{\epsilon_i \kappa_i A_i}{N_i} - \frac{\epsilon_i \kappa_i A_i X_i}{N_i Y_i} - \frac{\rho_i R_i}{S_i} - \frac{\pi_i A_i}{R_i} - \frac{\alpha_i I_i}{R_i} - \frac{\mu_{h_i} N_i}{S_i} \\ & + \textstyle\sum_{i=1}^{n} \frac{\epsilon_i \nu_i I_i}{N_i} - \frac{\epsilon_i \nu_i I_i X_i}{N_i Y_i} - \frac{\Psi_i}{X_i} - \frac{\eta_i Y_i}{Z_i} - \frac{\lambda_i E_i}{I_i} - \frac{\zeta_i E_i}{A_i} \\ & + \textstyle\sum_{i=1}^{n} 5\mu_{h_i} + \Psi_i + \eta_i + 3\mu_{v_i} - \mu_{v_i} X_i - \mu_{v_i} Y_i - \mu_{v_i} Z_i \\ & + \tfrac{1}{2}\left(\sigma_S^2 + \sigma_E^2 + \sigma_I^2 + \sigma_A^2 + \sigma_R^2\right)\end{aligned}$$

By (2.4) we assert that $(S_i(s), E_i(s), I_i(s), A_i(s), R_i(s),)_{i=1,\cdots,n} \in (0, \frac{\mathbf{\Gamma}_i}{\varphi})$ for all $s \in [0, t \wedge \tau_m]$ a.s . Hence $\sum_{i=1}^{n} \frac{\epsilon_i b_i Z_i}{N_i} < \frac{\mathbf{\Gamma}_i}{\varphi}$, $\sum_{i=1}^{n} \frac{\epsilon_i \kappa_i A_i}{N_i} < \frac{\mathbf{\Gamma}_i}{\varphi}$ and $\sum_{i=1}^{n} \frac{\epsilon_i \kappa_i I_i}{N_i} < \frac{\mathbf{\Gamma}_i}{\varphi}$,

therefore

$$\begin{aligned}\mathcal{L}V \leq \; & \textstyle\sum_{i=1}^{n} \frac{\mathbf{3\Gamma}_i}{\varphi} + \mu_{h_i} N_i + \zeta_i + \lambda_i + \rho_i + \alpha_i + \delta_i + \pi_i + 5\mu_{h_i} + \Psi_i + \eta_i + 3\mu_{v_i} \\ & + \tfrac{1}{2}\left(\sigma_S^2 + \sigma_E^2 + \sigma_I^2 + \sigma_A^2 + \sigma_R^2\right) =: D\end{aligned}$$

Denote by $\xi = \min(\tau_m, T)$, then

$$\int_0^{\xi} dV(S_i(s), E_i(s), I_i(s), R_i(s), A_i(s), X_i(s), Y_i(s)) \leq \int_0^{\xi} D ds + H(\xi),$$

where

$$\begin{aligned}H(s) = \; & \textstyle\int_0^s (S(u) - 1)\sigma_S dW_S(u) + \int_0^s (E(u) - 1)\sigma_E dW_E(u) + \int_0^s (I(u) - 1)\sigma_I dW_I(u) \\ & + \textstyle\int_0^s (A(u) - 1)\sigma_A dW_A(u) + \int_0^s (R(u) - 1)\sigma_R dW_R(u).\end{aligned}$$

Taking expectation, yields

$$\begin{aligned}& \mathbb{E}\left[V\left(S_i(\xi), E_i(\xi), I_i(\xi), A_i(\xi), R_i(\xi), X_i(\xi), Y_i(\xi), Z_i(\xi)\right)\right] \\ & \leq V\left(S_i(0), E_i(0), I_i(0), A_i(0), R_i(0), X_i(s), Y_i(s)\right) + \mathbb{E}\textstyle\int_0^{\xi} D ds \\ & \leq V\left(S_i(0), E_i(0), I_i(0), A_i(0), R_i(0), X_i(s), Y_i(s)\right) + DT.\end{aligned}$$

Set $\Omega_m = \{\omega \in \Omega : \tau_m < T\}$ for each $m \geq m_1$ and from equation (2.5), we have $\mathbb{P}(\Omega_m) \geq \epsilon$. Note that for every $\nu \in \Omega_m$, with these two bounds yield we get

$$\left\{S_i(\tau_m, \nu), E_i(\tau_m, \nu), I_i(\tau_m, \nu), A_i(\tau_m, \nu), R_i(\tau_m, \nu)\right\} \cap [m, \frac{1}{m}] \neq \emptyset.$$

Consequently,

$$V\left((S_i(\xi), E_i(\xi), I_i(\xi), A_i(\xi), R_i(\xi))_{i=1,\cdots,n}\right) \geq U_m$$

where

$$U_m = \min_{u \in \{1, a_0\}} \left\{m - u - u \ln \frac{m}{u}, \frac{1}{m} - u - u \ln \frac{1}{um}\right\}.$$

choose $a_0 > 0$ sufficiently small. Then we obtain

$$\begin{aligned}& V\left((S_i(0), E_i(0), I_i(0), A_i(0), R_i(0), X_i(s), Y_i(s))_{i=1,\cdots,n}\right) + DT \\ & \geq \mathbb{E}(1_{\Omega_m} V\left((S_i(\xi), E_i(\xi), I_i(\xi), A_i(\xi), R_i(\xi))_{i=1,\cdots,n}\right) \geq \epsilon U_m.\end{aligned}$$

Letting $m \to \infty$ leads to the contradiction $\infty = V\left((S_i(0), E_i(0), I_i(0), A_i(0), R_i(0))_{i=1,\cdots,n}\right) + DT < \infty$. Thus, as $\tau_m \geq \tau_\infty$, then $\tau_m = \tau_\infty = \infty$ a.s. This completes the proof. □

3 Basic Reproduction Number

The basic reproduction number, denoted by $\mathcal{R}_0$, is defined as the average number of secondary infections that occur when one infective is introduced into a completely susceptible host population (see [38] for instance).

To evaluate $\mathcal{R}_0$, we need to determine the model's disease free equilibrium points which are given by the solutions of the following system

$$\begin{cases} \Gamma_i - \left(\mu_{h_i} + \sum_{j\neq i=1}^{n} \psi_{i,j}^{S}\right) S_i + \sum_{j\neq i=1}^{n} \psi_{j,i}^{S} S_j = 0, \\ \\ -(\rho_i + \mu_{h_i}) R_i + \sum_{j\neq i=1}^{n} \psi_{j,i}^{R} R_j - \left(\sum_{j\neq i=1}^{n} \psi_{i,j}^{R}\right) R_i = 0, \\ \\ \Psi_i - \mu_{v_i} X_i = 0, \end{cases}$$

We obtain $X_i = \frac{\Psi_i}{\mu_{v_i}}$, and

$$\begin{cases} \sum_{j=1}^{n} \varphi_{i,j}^{S} S_j = \Gamma_i \\ \sum_{j=1}^{n} \varphi_{i,j}^{R} R_j = 0, \end{cases} \tag{3.6}$$

where

$$\begin{cases} \varphi_{i,j}^{Q} = -\psi_{i,j}^{Q} \text{ for } Q = S, R \text{ and } j = 1, \cdots, n, \ j \neq i \\ \varphi_{i,j}^{S} = \mu_{h_i} + \sum_{j\neq i=1}^{n} \psi_{i,j}^{S} \text{ and } \varphi_{i,j}^{R} = \rho_i + \mu_{h_i} + \sum_{j\neq i=1}^{n} \psi_{i,j}^{R} \text{ for } j = i. \end{cases}$$

Using matricial form, equation (3.6) reads as

$$\begin{cases} \varphi^{S} S = \Gamma \\ \varphi^{R} R = 0 \end{cases} \tag{3.7}$$

where $\varphi^{Q} = \left(\varphi_{i,j}^{Q}\right)_{1\leq i,j\leq 1}$, $S = (S_1, \cdots S_n)^{\top}$, $R = (R_1, \cdots R_n)^{\top}$ and $\Gamma = (\Gamma_1, \cdots \Gamma_n)^{\top}$.
It can be shown that the matrix φ^{Q} is an invertible Z-matrix in which the off-diagonal entries are nonzero,implying that system (3.7) has a unique solution $R = 0$ and $S = S^0 = \left(\varphi^{S}\right)^{-1} \Gamma$.
Thus, model (2.2) has a unique disease free equilibrium point

$$\mathcal{E}_0 = \left(\left(S_i^0\right)_{i=1,\cdots,n}, \mathbf{0}, \mathbf{0}, \mathbf{0}, \mathbf{0}, \left(X_i^0\right)_{i=1,\cdots,n}, \mathbf{0}, \mathbf{0}\right)$$

where $\mathbf{0} = (\underbrace{0, \cdots, 0}_{n \text{ times}})$, $\left(X_i^0\right)_{i=1,\cdots,n} = \left(\frac{\Psi_i}{\mu_{v_i}}\right)_{i=1,\cdots,n}$ and $\left(S_i^0\right)_{i=1,\cdots,n} = \left(\varphi^{S}\right)^{-1} \Gamma$.
We are now in a position to compute $\mathcal{R}_0$ for the deterministic counterpart of the stochastic model2.2 by following the approach of Van den Driessche and Watmough since the model satisfies the hypotheses as set out in [38]. The model's disease compartments are E_i, I_i, A_i, Y_i and Z_i.
First we rewrite the equations for the model's infected classes

$$(E_1, \cdots, E_n, I_1, \cdots, I_n, A_1, \cdots, A_n, Y_1, \cdots, Y_n, Z_1, \cdots, Z_n)$$

as

$$\begin{cases} \dfrac{dE_i}{dt} = \Lambda_i S_i - \sum_{j=1}^{n} \varphi_{i,j}^{E} E_j \\ \dfrac{dI_i}{dt} = \lambda_i E_i - \sum_{j=1}^{n} \varphi_{i,j}^{I} I_j \\ \dfrac{dA_i}{dt} = \zeta_i E_i - \sum_{j=1}^{n} \varphi_{i,j}^{A} A_j \\ \dfrac{dY_i}{dt} = \beta_i X_i - (\eta_i + \mu_{v_i}) Y_i \\ \dfrac{dZ_i}{dt} = \eta_i Y_i - \mu_{v_i} Z_i \end{cases}$$

where

$$\begin{cases} \varphi_{i,j}^{Q} = -\psi_{i,j}^{Q} \text{ for } Q = E, I \text{ or } A \text{ and } j = 1, \cdots, n \; j \neq i \\ \varphi_{i,i}^{E} = \lambda_i + \zeta_i + \mu_{h_i} + \sum_{j \neq i=1}^{n} \psi_{i,j}^{E}, \\ \varphi_{i,i}^{I} = \alpha_i + \delta_i + \mu_{h_i} + \sum_{j \neq i=1}^{n} \psi_{i,j}^{I}, \\ \varphi_{i,i}^{A} = \pi_i + \mu_{h_i} + \sum_{j \neq i=1}^{n} \psi_{i,j}^{A} \end{cases}.$$

With these notations the vector of the rates of new infections and the vector of the ratres of other transfers between disease states are respectively given by

$$\mathcal{F}(x) = \begin{bmatrix} \left[\dfrac{\epsilon_i b_i Z_i S_i}{S_i + E_i + I_i + A_i + R_i} \right]_{i=1,\cdots,n} \\ 0_n \\ 0_n \\ \left[\dfrac{\epsilon_i \kappa_i A_i X_i + \epsilon_i \nu_i I_i X_i}{S_i + E_i + I_i + A_i + R_i} \right]_{i=1,\cdots,n} \\ 0_n \end{bmatrix}, \text{ and } \mathcal{V}(x) = \begin{bmatrix} \left[\sum_{j=1}^{n} \varphi_{i,j}^{E} E_j \right]_{i=1,\cdots,n} \\ \left[-\lambda_i E_i + \sum_{j=1}^{n} \varphi_{i,j}^{I} I_j \right]_{i=1,\cdots,n} \\ \left[-\zeta_i E_i + \sum_{j=1}^{n} \varphi_{i,j}^{A} A_j \right]_{i=1,\cdots,n} \\ [(\eta_i + \mu_{v_i}) Y_i]_{i=1,\cdots,n} \\ [-\eta_i Y_i + \mu_{v_i} Z_i]_{i=1,\cdots,n} \end{bmatrix}.$$

The Jacobian matrices of $\mathcal{F}$ and $\mathcal{V}$ with respect to infected classes (E_i, I_i, A_i , Y_i, and Z_i) evaluated at the disease free equilibrium point $\mathcal{E}_0$ are respectively given by

$$F = \begin{bmatrix} \mathbb{O} & \mathbb{O} & \mathbb{O} & \mathbb{O} & F_{1,5} \\ \mathbb{O} & \mathbb{O} & \mathbb{O} & \mathbb{O} & \mathbb{O} \\ \mathbb{O} & \mathbb{O} & \mathbb{O} & \mathbb{O} & \mathbb{O} \\ \mathbb{O} & F_{4,2} & F_{4,3} & \mathbb{O} & \mathbb{O} \\ \mathbb{O} & \mathbb{O} & \mathbb{O} & \mathbb{O} & \mathbb{O} \end{bmatrix} \text{ and } V = \begin{bmatrix} V_{1,1} & \mathbb{O} & \mathbb{O} & \mathbb{O} & \mathbb{O} \\ V_{2,1} & V_{2,2} & \mathbb{O} & \mathbb{O} & \mathbb{O} \\ V_{3,1} & \mathbb{O} & V_{3,3} & \mathbb{O} & \mathbb{O} \\ \mathbb{O} & \mathbb{O} & \mathbb{O} & V_{4,4} & \mathbb{O} \\ \mathbb{O} & \mathbb{O} & \mathbb{O} & V_{5,4} & V_{5,5} \end{bmatrix}$$

where

$$\begin{cases} F_{1,4} = diag\left\{\epsilon_1 b_1, \epsilon_2 b_2, \cdots, \epsilon_n b_n\right\} \\ F_{4,2} = diag\left\{\epsilon_1 \nu_1 \dfrac{X_1^0}{S_1^0}, \epsilon_2 \nu_2 \dfrac{X_2^0}{S_2^0}, \cdots, \epsilon_n \kappa_n \dfrac{X_n^0}{S_n^0}\right\} \\ F_{4,3} = diag\left\{\epsilon_1 \kappa_1 \dfrac{X_1^0}{S_1^0}, \epsilon_2 \kappa_2 \dfrac{X_2^0}{S_2^0}, \cdots, \epsilon_n \kappa_n \dfrac{X_n^0}{S_n^0}\right\} \end{cases}$$

and

$$\begin{cases} V_{1,1} = \left(\varphi^E_{i,j}\right)_{1\leq i,j\leq n} \\ V_{2,1} = diag\left(-\lambda_1, \cdots, -\lambda_n\right) \\ V_{2,2} = \left(\varphi^I_{i,j}\right)_{1\leq i,j\leq n} \\ V_{3,1} = diag\left(-\zeta_1, \cdots, -\zeta_n\right) \\ V_{3,3} = \left(\varphi^A_{i,j}\right)_{1\leq i,j\leq n} \\ V_{4,4} = diag\left(\eta_1+\mu_{v_1}, \cdots, \eta_n+\mu_{v_n}\right) \\ V_{5,4} = diag\left(-\eta_1, \cdots, -\eta_n\right) \\ V_{5,5} = diag\left(\mu_{v_1}, \cdots, \mu_{v_n}\right) \end{cases}$$

and $\mathbb{O}$ is the n by n matrix with all entries being equal to 0.
The matrix F is a non-negative matrix of rank one and can be written as the product of vectors. Matrices $V_{1,1}, V_{2,2}, V_{3,3}, V_{4,4}$ and $V_{5,5}$ are irreducible non-singular M-matrix and thus their inverses are

$$V^{-1} = \begin{bmatrix} V_{1,1}^{-1} & \mathbb{O} & \mathbb{O} & \mathbb{O} & \mathbb{O} \\ -V_{2,2}^{-1}V_{2,1}V_{1,1}^{-1} & V_{2,2}^{-1} & \mathbb{O} & \mathbb{O} & \mathbb{O} \\ -V_{3,3}^{-1}V_{3,1}V_{1,1}^{-1} & \mathbb{O} & V_{3,3}^{-1} & \mathbb{O} & \mathbb{O} \\ \mathbb{O} & \mathbb{O} & \mathbb{O} & V_{4,4}^{-1} & \mathbb{O} \\ \mathbb{O} & \mathbb{O} & \mathbb{O} & -V_{5,5}^{-1}V_{5,4}V_{4,4}^{-1} & V_{5,5}^{-1} \end{bmatrix}$$

The Next Generation Matrix is given by:

$$M = FV^{-1} = \begin{bmatrix} \mathbb{O} & \mathbb{O} & \mathbb{O} & M_{1,4} & M_{1,5} \\ \mathbb{O} & \mathbb{O} & \mathbb{O} & \mathbb{O} & \mathbb{O} \\ \mathbb{O} & \mathbb{O} & \mathbb{O} & \mathbb{O} & \mathbb{O} \\ M_{4,1} & M_{4,2} & M_{4,3} & \mathbb{O} & \mathbb{O} \\ \mathbb{O} & \mathbb{O} & \mathbb{O} & \mathbb{O} & \mathbb{O} \end{bmatrix}$$

where

$$\begin{cases} M_{1,4} := F_{1,4}V_{4,4}^{-1}V_{5,4}V_{5,5}^{-1}, \\ M_{1,5} := F_{1,4}V_{5,5}^{-1}, \\ M_{4,1} := F_{4,2}V_{1,1}^{-1}V_{2,1}V_{2,2}^{-1} + F_{4,3}V_{1,1}^{-1}V_{3,1}V_{3,3}^{-1} \\ M_{4,2} := F_{4.2}V_{2.2}^{-1} \\ M_{4,3} := F_{4.3}V_{3.3}^{-1}. \end{cases}$$

Hence, the basic reproduction number $\mathcal{R}_0$ given by the spectral radius of FV^{-1}, is

$$\mathcal{R}_0 = \rho\left(B\right)$$

where B is the $n \times n$ positive matrix given by

$$B = M_{1,4}M_{4,1} = F_{1,4}V_{4,4}^{-1}V_{5,4}V_{5,5}^{-1}\left(F_{4,2}V_{1,1}^{-1}V_{2,1}V_{2,2}^{-1} + F_{4,3}V_{1,1}^{-1}V_{3,1}V_{3,3}^{-1}\right).$$

$$F_{1,4}V_{4,4}^{-1}V_{5,4}V_{5,5}^{-1} = diag\left(\frac{-\epsilon_1 b_1\eta_1}{\mu_{v_1}\left(\eta_1+\mu_{v_1}\right)}, \cdots, \frac{-\epsilon_n b_n\eta_n}{\mu_{v_n}\left(\eta_n+\mu_{v_n}\right)}\right)$$

$$F_{4,2}V_{1,1}^{-1}V_{2,1}V_{2,2}^{-1} = diag\left\{\epsilon_1\nu_1\frac{X_1^0}{S_1^0}, \cdots, \epsilon_n\kappa_n\frac{X_n^0}{S_n^0}\right\}\left(\varphi^E\right)^{-1} diag\left(-\lambda_1, \cdots, -\lambda_n\right)\left(\varphi^I\right)^{-1}$$

$$F_{4,3}V_{1,1}^{-1}V_{3,1}V_{3,3}^{-1} = diag\left\{\epsilon_1\kappa_1\frac{X_1^0}{S_1^0}, \cdots, \epsilon_n\kappa_n\frac{X_n^0}{S_n^0}\right\}\left(\varphi^E\right)^{-1} diag\left(-\zeta_1, \cdots, -\zeta_n\right)\left(\varphi^A\right)^{-1}$$

Clearly, the calculation of $\rho(B)$ involves the inversion of n by n matrices which can lead to some tedious calculations when n is large. We discuss the following particular cases:

- **Case 1:** No movement between patches, if we ignore population movement between patches, that is $\psi_{i,j}^{Q} = \psi_{j,i}^{Q} = 0$ for $j = 1, \cdots, n$ $j \neq i$ and $Q = E, I$ or A, we have

$$\begin{cases} \varphi_{i,j}^{Q} = 0 \text{ for } j = 1, \cdots, n \; j \neq i \text{ and } Q = E, I \text{ or } A \\ \varphi_{i,i}^{E} = \lambda_i + \zeta_i + \mu_{h_i}, \varphi_{i,i}^{I} = \alpha_i + \delta_i + \mu_{h_i}, \varphi_{i,i}^{A} = \pi_i + \mu_{h_i}. \end{cases}$$

  Then

$$\begin{aligned} F_{1,4}V_{4,4}^{-1}V_{5,4}V_{5,5}^{-1} &= diag\left(\frac{-\epsilon_1 b_1 \eta_1}{\mu_{v_1}(\eta_1+\mu_{v_1})}, \cdots, \frac{-\epsilon_n b_n \eta_n}{\mu_{v_n}(\eta_n+\mu_{v_n})}\right) \\ F_{4,2}V_{1,1}^{-1}V_{2,1}V_{2,2}^{-1} &= diag\left\{-\lambda_1\epsilon_1\nu_1\frac{X_1^0}{S_1^0\varphi_{11}^E\varphi_{11}^I}, \cdots, -\lambda_n\epsilon_n\nu_n\frac{X_n^0}{S_n^0\varphi_{nn}^E\varphi_{nn}^I}\right\} \\ F_{4,3}V_{1,1}^{-1}V_{3,1}V_{3,3}^{-1} &= diag\left\{-\zeta_1\epsilon_1\kappa_1\frac{X_1^0}{S_1^0\varphi_{11}^E\varphi_{11}^A}, \cdots, -\zeta_n\epsilon_n\kappa_n\frac{X_n^0}{S_n^0\varphi_{nn}^E\varphi_{nn}^A}\right\} \end{aligned}$$

  Therefore

$$B = diag\left\{\frac{\epsilon_1^2 b_1\eta_1 X_1^0}{\mu_{v_1}(\eta_1+\mu_{v_1})S_1^0\varphi_{11}^E}\left(\frac{\lambda_1\nu_1}{\varphi_{11}^I}+\frac{\zeta_1\kappa_1}{\varphi_{11}^A}\right), \cdots, \frac{\epsilon_n^2 b_n\eta_n X_n^0}{\mu_{v_n}(\eta_n+\mu_{v_n})S_n^0\varphi_{nn}^E}\left(\frac{\lambda_n\nu_n}{\varphi_{nn}^I}+\frac{\zeta_n\kappa_n}{\varphi_{nn}^A}\right)\right\}.$$

  Hence

$$\mathcal{R}_0 = \max \mathcal{R}_{0i}$$

  where

$$\mathcal{R}_{0i} = \frac{\epsilon_i^2 b_i\eta_i X_i^0}{\mu_{v_i}(\eta_i+\mu_{v_i})(\lambda_i+\zeta_i+\mu_{h_i})S_i^0}\left(\frac{\lambda_i\nu_i}{\alpha_i+\delta_i+\mu_{h_i}}+\frac{\zeta_i\kappa_i}{\pi_i+\mu_{h_i}}\right).$$

  Thus if $\mathcal{R}_{0i} > 1$ for all i, then the disease-free equilibrium (DFE) is unstable leading and the disease may invade the population, but if $\mathcal{R}_{0i} < 1$ for all i, then DFE is locally asymptotically stable and the disease may be eliminated.
  Thus, it is important to reduce $\mathcal{R}_{0i}$ in every patch i for the disease to be controlled.

- **Case 2:** Two-patch model with movement, in the case of nonzero rates of population's movement, we consider a situation where the whole population is divided in two (large) patches only, that is $n = 2$, then we have

$$\begin{cases} F_{1,4} = diag\{\epsilon_1 b_1, \epsilon_2 b_2\} \\ F_{4,2} = diag\left\{\epsilon_1\nu_1\frac{X_1^0}{S_1^0}, \epsilon_2\nu_2\frac{X_2^0}{S_2^0}\right\} \\ F_{4,3} = diag\left\{\epsilon_1\kappa_1\frac{X_1^0}{S_1^0}, \epsilon_2\kappa_2\frac{X_2^0}{S_2^0}\right\} \end{cases}$$

and

$$\begin{cases} V_{1,1} = \left(\varphi_{i,j}^{E}\right)_{1\leq i,j\leq 2} \\ V_{2,1} = diag\left(-\lambda_1, -\lambda_2\right) \\ V_{2,2} = \left(\varphi_{i,j}^{I}\right)_{1\leq i,j\leq 2} \\ V_{3,1} = diag\left(-\zeta_1, -\zeta_2\right) \\ V_{3,3} = \left(\varphi_{i,j}^{A}\right)_{1\leq i,j\leq 2} \\ V_{4,4} = diag\left(\eta_1+\mu_{v_1}, \eta_2+\mu_{v_2}\right) \\ V_{5,4} = diag\left(-\eta_1, -\eta_2\right) \\ V_{5,5} = diag\left(\mu_{v_1}, \mu_{v_2}\right) \end{cases}$$

Then

$$B = F_{1,4}V_{4,4}^{-1}V_{5,4}V_{5,5}^{-1}\left(F_{4,2}V_{1,1}^{-1}V_{2,1}V_{2,2}^{-1} + F_{4,3}V_{1,1}^{-1}V_{3,1}V_{3,3}^{-1}\right) = \begin{bmatrix} B_{11} & B_{12} \\ B_{21} & B_{22} \end{bmatrix}$$

where

$$\begin{cases} B_{11} = \frac{-\epsilon_1 b_1 \eta_1}{\mu_{v_1}\left(\eta_1+\mu_{v_1}\right)\left(\left(\varphi_{12}^{E}\right)^2+\varphi_{11}^{E}\varphi_{22}^{E}\right)}\left(\frac{\nu_1\epsilon_1\left(\lambda_2\varphi_{12}^{E}\varphi_{12}^{I}-\lambda_1\varphi_{11}^{E}\varphi_{11}^{I}\right)}{\left(\varphi_{12}^{I}\right)^2+\varphi_{11}^{I}\varphi_{22}^{I}} + \frac{\kappa_1\epsilon_1\left(\zeta_2\varphi_{12}^{E}\varphi_{12}^{A}-\zeta_1\varphi_{11}^{E}\varphi_{11}^{A}\right)}{\left(\varphi_{12}^{A}\right)^2+\varphi_{11}^{A}\varphi_{22}^{A}}\right) \\ B_{12} = \frac{\epsilon_1 b_1 \eta_1}{\mu_{v_1}\left(\eta_1+\mu_{v_1}\right)\left(\left(\varphi_{12}^{E}\right)^2+\varphi_{11}^{E}\varphi_{22}^{E}\right)}\left(\frac{\nu_1\epsilon_1\left(\lambda_1\varphi_{11}^{E}\varphi_{12}^{I}+\lambda_2\varphi_{12}^{E}\varphi_{22}^{I}\right)}{\left(\varphi_{12}^{I}\right)^2+\varphi_{11}^{I}\varphi_{22}^{I}} + \frac{\kappa_1\epsilon_1\left(\zeta_1\varphi_{11}^{E}\varphi_{12}^{A}+\zeta_2\varphi_{12}^{E}\varphi_{22}^{A}\right)}{\left(\varphi_{12}^{A}\right)^2+\varphi_{11}^{A}\varphi_{22}^{A}}\right) \\ B_{21} = \frac{-\epsilon_2 b_2 \eta_2}{\mu_{v_2}(\eta_2+\mu_{v2})\left(\left(\varphi_{12}^{E}\right)^2+\varphi_{11}^{E}\varphi_{22}^{E}\right)}\left(\frac{\nu_2\epsilon_2\left(\lambda_1\varphi_{12}^{E}\varphi_{11}^{I}+\lambda_2\varphi_{22}^{E}\varphi_{12}^{I}\right)}{\left(\varphi_{12}^{I}\right)^2+\varphi_{11}^{I}\varphi_{22}^{I}} + \frac{\kappa_2\epsilon_2\left(\zeta_1\varphi_{12}^{E}\varphi_{11}^{A}+\zeta_2\varphi_{22}^{E}\varphi_{12}^{A}\right)}{\left(\varphi_{12}^{A}\right)^2+\varphi_{11}^{A}\varphi_{22}^{A}}\right) \\ B_{22} = \frac{-\epsilon_2 b_2 \eta_2}{\mu_{v_2}(\eta_2+\mu_{v2})\left(\left(\varphi_{12}^{E}\right)^2+\varphi_{11}^{E}\varphi_{22}^{E}\right)}\left(\frac{\nu_2\epsilon_2\left(\lambda_1\varphi_{12}^{E}\varphi_{12}^{I}-\lambda_2\varphi_{22}^{E}\varphi_{22}^{I}\right)}{\left(\varphi_{12}^{I}\right)^2+\varphi_{11}^{I}\varphi_{22}^{I}} + \frac{\kappa_2\epsilon_2\left(\zeta_1\varphi_{12}^{E}\varphi_{12}^{A}-\zeta_2\varphi_{22}^{E}\varphi_{22}^{A}\right)}{\left(\varphi_{12}^{A}\right)^2+\varphi_{11}^{A}\varphi_{22}^{A}}\right) \end{cases}$$

Hence

$$R_0 = \frac{1}{2}\left(B_{11} + B_{22} + \sqrt{\left(B_{11} - B_{22}\right)^2 + 4B_{12}B_{21}}\right)$$

To understand the effects of people's movement on $\mathcal{R}_0$, one can investigate the variation of $\mathcal{R}_0$ with respect to the immigration parameters φ_{12}^{E}, φ_{12}^{A} and φ_{12}^{I}. However, even in this simple case of two patches the derivatives of $\mathcal{R}_0$ with respect to these parameters are too complex to explore analytically.

One of the interventioins that are aimed at reducing $\mathcal{R}_{0i}$ is the Long-lasting insecticide treated nets (LLINs) which mainly reduce the contact between humans and mosquitoes. Implementing this intervenuion in our model can be expressed by $(1-\chi V)\epsilon$ where χ is the proportion of LLINs coverage and V is the effectiveness of vector control. These two parameters are estimated using the data fitting process. It is worth noting that the basic reproduction number of the deterministic model is closely related to that of the stochastic model which is dependent on the initial number of infectious individuals for each patch i.

4 Model fitting and simulations

We restrict our model simulations and data fitting to the three safest zones of Equatorial region: Central Equatoria State(CES), Bahr El Ghazal region: Western Bahr El Ghazal State(WBGZ)) and Upper Nile region : Warrap State(WRP). By doing so, we are assuming that movements from and into other regions are negligible compared to those from these three main regions. Basically, this turns out to considering the three regions together as a closed system, whereby only movements within and between these three regions are considered. Our stochastic model is fitted to weekly malaria data of 2011 from these three regions (shown in Figure 3) using the maximum likelihood approach. The model is run deterministically from the year 2000 to reach a steady state before being fitted to data from the year 2011. We assume that weekly malaria data were reported according to a Poisson process with reporting rate γ. Since the reporting rate is incomplete we assume it to be no more than 85%. Data are cases of malaria from the National Malaria Indicator Survey (MIS) of South Sudan, see S1 Dataset. Estimates of the population in each selected State in the year 2009 was based on the pre-independence national census of 2008 [34].

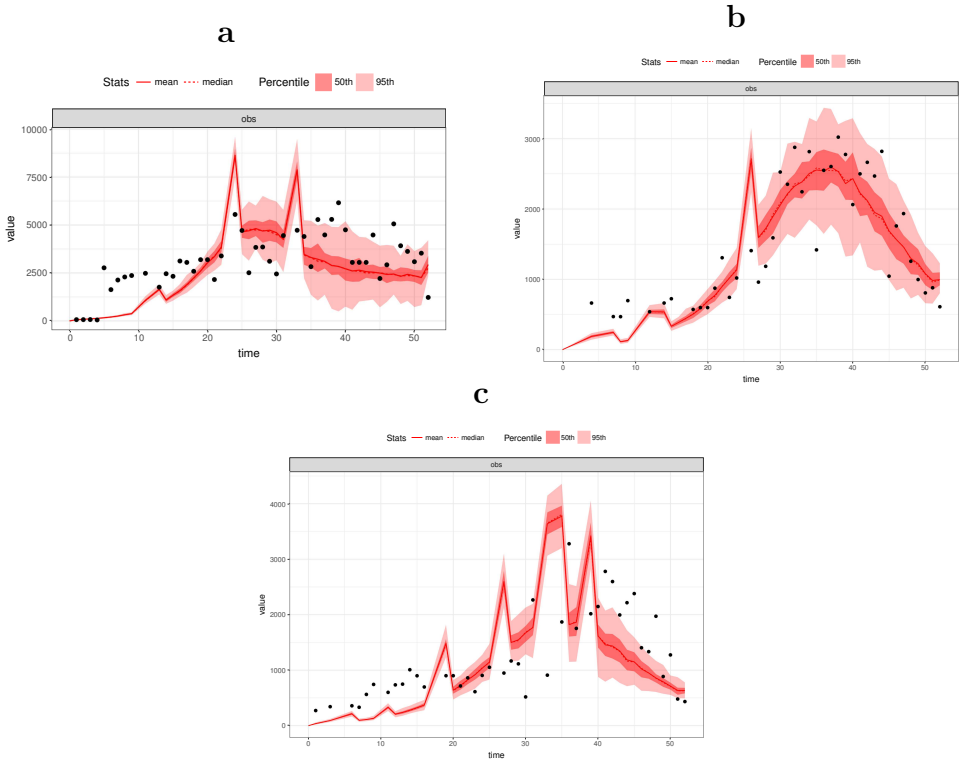

Figure 3: Illustration of the model fitting: the model assessment (line) run against data (dots) of CES (a), WBGZ (b) and WRP (c) for 2011, attached with the parameters estimated during fitting process in Table 3, along with the time-series of the extinction probability (i.e. the proportion of faded out simulations).

We describe the stochastic SEIAR model with Poisson observation and constant population size. We simulate and fit the model to data using the "fitR" package which takes the "fitmodel" object as a list that stores variables and functions. These arguments are model name, character vector of state variables, character vector of parameters, R-function to simulate forward the model, R-function that evaluates the likelihood of the provided data, R-function to generate observation from a model simulation and *ssa.adaptivetau* function which takes a vector of initial conditions, the list of transitions and rate function, a named vector of parameters, and the final time.

According to continuous Markov processes theory, a Langevin equation can be described in the white-noise form [16]. The proposed SDE is considered to be a Langevin equation that is driven by zero-mean Gaussian noise and hence describes the *tau-leaping*. We compute a Monte-Carlo estimate of the log-likelihood of parameters for a stochastic model defined in a *fitmodel* object that takes values of the parameters, initial values of the state variables, observation times and observed data and number of particles.

We add a new stage variable (Inc) onto the model to track the daily number of new cases, assuming that these new cases are reported when they become symptomatic or infectious. In order for the model to predict incidence of malaria cases, we use the simulation function of the model with the initial state and given parameters calibrated with $x_{i,j}, (i = 1, ..., n; j = 1, ..., m)$ as the observed weekly malaria cases for state j during week i. Calculating the likelihood of each data point $x_{i,j}$ taking its observed cases and evaluating it with respect to a Poisson distribution centred around the model point. We assume that the Poisson probability of observing x_i IID (Independent and Identically Distributed) counts with unknow parameter θ. A description of the method of data-fitting is provided in S2 Appendix.

$$X|\theta \sim Poisson(\theta)$$

The likelihood function is:

$$\begin{aligned} L\left(\theta|x_1, x_2, \cdots, x_n\right) &= p\left(X = x_1|\theta\right) p\left(X = x_2|\theta\right) \cdots p\left(X = x_n|\theta\right) \\ &= \frac{e^{-\theta}\theta^{x_1 x_2 \cdots x_n}}{x_1! x_2! \cdots x_n!} = \prod_{i=1}^{n} \frac{e^{-\theta}\theta^{x_i}}{x_i!} \end{aligned}$$

and the log likelihood function becomes

$$\ln\left(L\left(\theta|x_1, x_2, \cdots, x_n\right)\right) = -n\theta + \left(\sum_{i=1}^{n} x_i\right) \ln\theta - \ln(\prod_{i=1}^{n} x_i!)$$

The model is fitted to three patch dataset. Considering an IID sample $x_{i,j}$ for patch j from a Poisson variable the log likelihood to be maximised as

$$\ln\left(L\left(\theta_j|x_{i,j}\right)\right) = \sum_{i=1}^{n}\sum_{j=1}^{3}\left(x_i\theta_j - \theta_j\right)$$

We visually assess a model run against data using a stochastic simulation algorithm, which generates an observation trajectory from the model, parameters and initial state

plots it (lines) against the data (points) of each patch using 1000 replicates simulation with 95% Confidence Interval (CI) constructed for each of the experiments.

Several model parameters (i.e, $\epsilon, b, \nu, \lambda, \zeta, \alpha, \rho$) are estimated during this fitting

Table 3: Model parameters estimated duraing the fitting process

Symbols	CES estimates	WBGZ estimates	WRP estimates	References
Γ	$0.0000514*N_1$	$0.0000514*N_2$	$0.0000514*N_3$	Estimated
N_i	N_1 =7983420	N_2 =9967450	N_3 =7826740	[34]
μ_h	0.0000514	0.0000514	0.0000514	Estimated
δ	0.00004	0.00004	0.00004	[6]
ϵ	36.6 (25.24, 50.4)	29.7 (20.2, 40.4)	32.5 (20.7, 45.31)	Estimated
b	0.84 (0.72, 0.94)	0.84 (0.72, 0.94)	0.84 (0.72, 0.94)	Estimated
ν	0.48	0.48	0.48	Estimated
κ	0.4	0.4	0.4	[39]
λ	0.2 (0.083, 0.25);	0.167 (0.083, 0.25)	0.167 (0.083, 0.25)	Estimated
ζ	0.0525	0.0525	0.0525	Estimated
α	1/16,	1/20,	1/18	Estimated
π	1/150	1/190	1/220	Estimated
ρ	1/25	1/20	1/37	Estimated
η	1/12	1/12	1/12	[6]
μ_v	0.04	0.04	0.04	[6]
Ψ	0.13	0.13	0.13	[28]

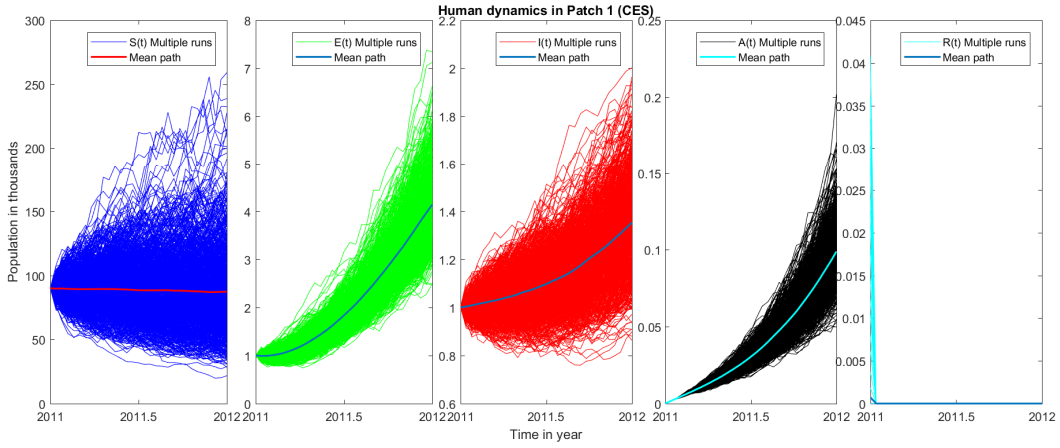

Figure 4: Simulation trajectory for the fitted model of human in thousands expressed in disease classification (S, E, I, A, R) for Patch 1 (CES), with $\sigma_S = 0.1, \sigma_E = 0.35, \sigma_I = 0.065, \sigma_A = 0.23$ and $\sigma_R = 0.45$.

process and those which are not estimated were collected from literature and are listed in Table 3. These parameters were assumed to be constant and were jointly estimated by utilizing fitR (version 0.1 [5]) and by plotting the mean and the median as well as the 95^{th} and 50^{th} percentiles of several replicated simulations. We assume an underlying Poisson distribution with a canonical vectors' parameter (representing a set of model parameters), θ, to be estimated. The resulting model fit of the observed measurement

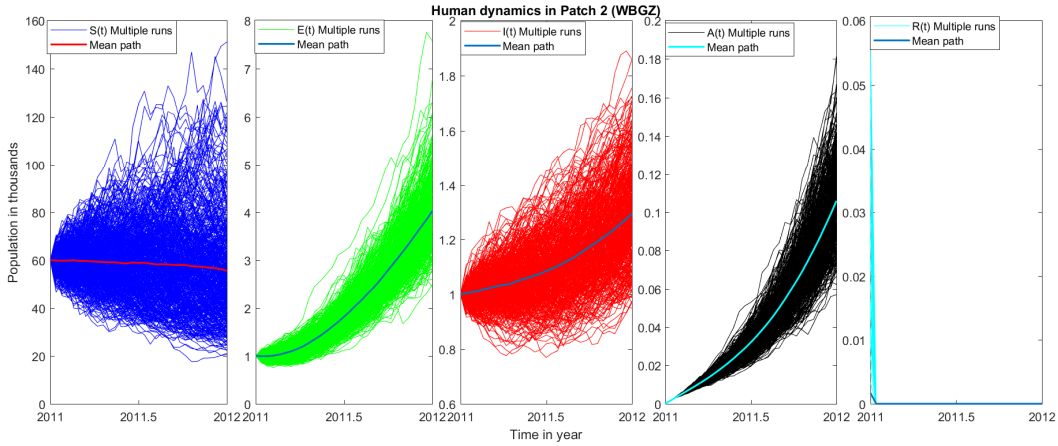

Figure 5: Simulation trajectory for the fitted model of human in thousands expressed in disease classification (S, E, I, A, R) for Patch 2 (WBGZ) with $\sigma_S = 0.1, \sigma_E = 0.35, \sigma_I = 0.065, \sigma_A = 0.23$ and $\sigma_R = 0.45$.

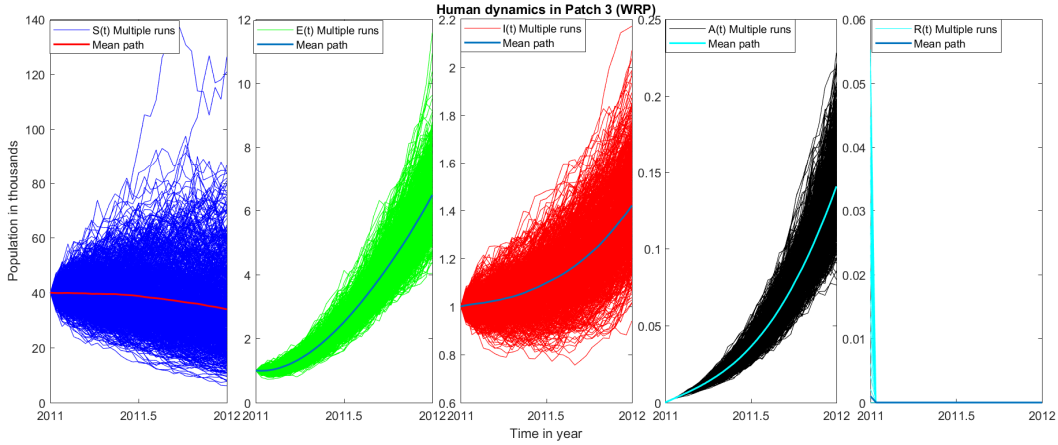

Figure 6: Simulation trajectory for the fitted model of human in thousands expressed in disease classification (S, E, I, A, R) for Patch 3 (WRP) with $\sigma_S = 0.1, \sigma_E = 0.35, \sigma_I = 0.065, \sigma_A = 0.23$ and $\sigma_R = 0.45$.

(the annual cases recorded) is shown in Figure 3.

Mobility rates are often difficult to estimate. However, obtaining information on the relative sizes of the migration parameters ($\Theta_i^Q = \sum_{j\neq i=1}^{n} \psi_{j,i}^Q Q(j) - \sum_{j\neq i=1}^{n} \psi_{i,j}^Q Q(i)$ with $Q = S, E, I, A$ and R and) may be appropriate to provide insight into where control measures should be applied. We assumed that the net inflow of migrants is greater than the net outflow ($\sum_{j\neq i=1}^{n} \psi_{j,i}^Q > \sum_{j\neq i=1}^{n} \psi_{i,j}^Q$). Migration parameters ψ_{ij}^Q and ψ_{ji}^Q were estimated as inverse of proportion of time for human moving to spend on patch j from patch i or on patch i from patch j. Subsequently, we use the estimated parameters along with some migration parameter values to simulate the model's projections for different values of the migration. We present the resulting graphs and their corresponding parameters in figures 7 and 8. The proposed metapopulation stochastic model accounts for random movement of people between patches and allows for the usage of bednets in n different patches. This provides us with some useful control strategies to regulate disease dynamics. Unlike determinstic models, the stochastic nature of this model allowed us to capture disease extinction in finite time, especially when the noise intensity is high.

5 Concluding remarks

In this paper we investigated the role of human mobility on malaria severity in South Sudan. We used a modified model of Mukhtar et al. [28] to carry out our investigation. The model is a metapopulation deterministic model consisting of three patches in three different regions of South Sudan. We incorporate a white noise in deterministic model to account for unpredictable population. The basic reproduction number $\mathcal{R}_0$, for metapopulation deterministic model, was calculated using the next generation matrix method. The threshold parameter, $\mathcal{R}_0$, is the expected number of humans and mosquitoes that would be infected with malaria by a single infected human/mosquito who had been introduced into disease-free population. A precise usage of $\mathcal{R}_0$, is to advise on the disease steady state of the considered patches. Another task in this study was to perform the model calibration. To this end, model parameter value estimates are determined to provide incidence case data (weekly cases data for the patches) for 2011.

We used a statistical approach, namely the maximum likelihood of Poisson distribution. Figure 3 illustrates the infectious class of the model fitted into data of three patches using the package fitR (version 0.1 [5]) and this include the mean, the median as well as the 95th and 50th percentiles of multiple replicated simulations.

We used simulation to generate an observation trajectory for the fitted model and also to demonstrate the population dynamics of humans (see Figures 4- 6). The predicted pattern of observation for a stochastic model with a variety of migration pattern was carried out, as shown in Figure 7 and 8. It turns out that malaria persists in the patches when there is human inflow in the patches although intervention coverage is as high as 75% (can be seen in the accompanying Table 4). However, the course of the disease in a low transmission area such as WRP (Patch 3 b) seems to go extinct. This implies that with an unprecedented number of people who are on the move (one out

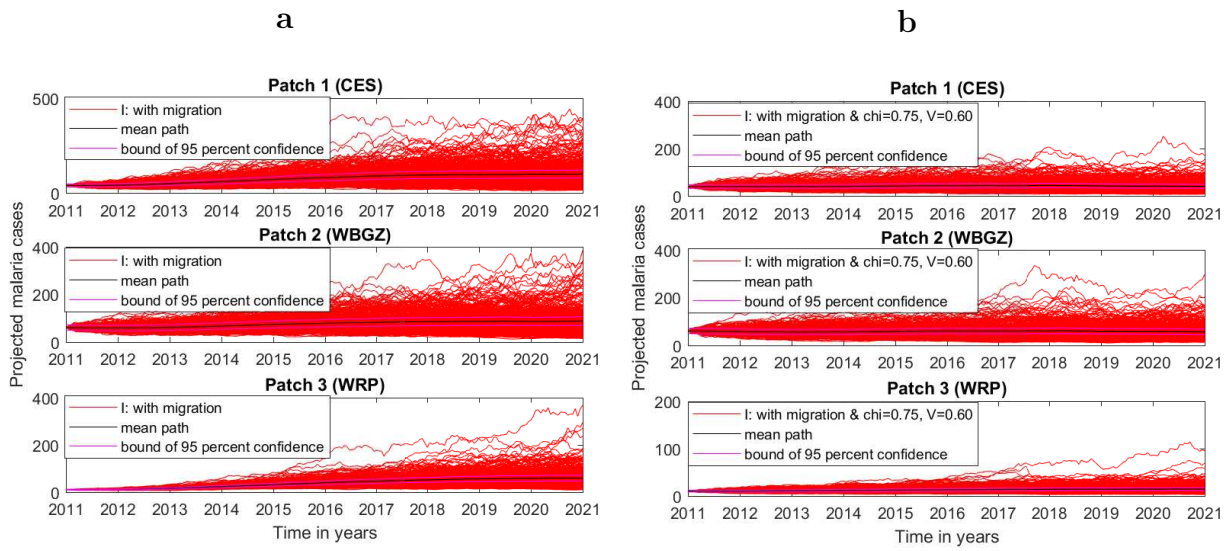

Figure 7: Projected cases of malaria (represented by the infectious class of the model) using parameter values in Table 3 assess the impact of movement between patches: migration rate: $\Theta_{CES} = (0.05, 0.0015, 0.0051, 0.061, 0.009)^Q$, $\Theta_{WBGZ} = (0.036, 0.0021, 0.008, 0.008, 0.056)^Q$ & $\Theta_{WRP} = (0.068, 0.0051, 0.0054, 0.02, 0.0053)^Q$, with no interventions of LLINs (a), with interventions of LLINs (b).

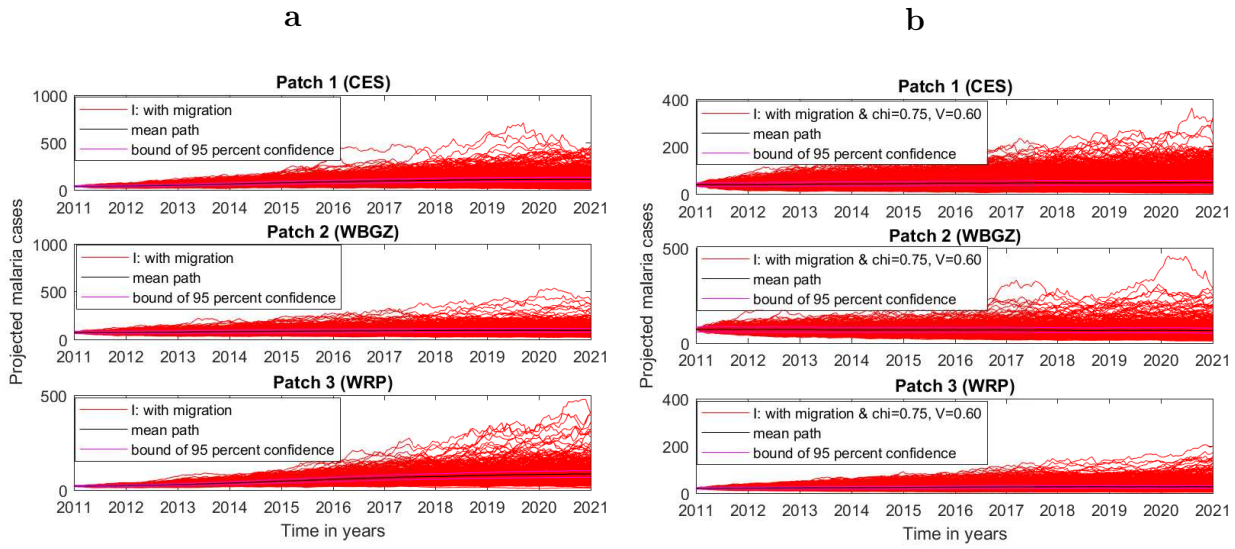

Figure 8: Features high migration rate at $\Theta_{CES} = (0.25, 0.035, 0.0415, 0.061, 0.0256)^Q$, $\Theta_{WBGZ} = (0.25, 0.051, 0.0215, 0.01, 0.056)^Q$ & $\Theta_{WRP} = (0.18, 0.012, 0.0185, 0.02, 0.046)^Q$, with no interventions of LLINs (a), with interventions of LLINs (b) for projected malaria cases.

of every five people in South Sudan have been forcibly displaced) can pose challenges to malaria control and elimination. Figure 9 demonstrates the correlation pattern of malaria disease with intervention coverage and intervention involving mobility. With the usage of threshold $\mathcal{R}_0$, the result indicated migration of a large number of people (the case of the conflict that leads to population pressure) and their circulation can favor malaria transmission (increase of $\mathcal{R}_0$) compared to less or no migration (see Figure 9). This confirms that human movement is one of the contributing factors to the resurgence of malaria, which can be explained by when infected individual move from areas where malaria was still endemic to malaria-free areas and also could happen when susceptible people move to malarious regions, they can increase their risk of acquiring the disease. It can be seen also from the result that human mobility is sufficient to preserve malaria disease firmness in the patches. We concluded that the responsiveness of malaria to the human mobility is high that can cause the implications on malaria control in South Sudan, and efforts to ameliorate health and monitoring of migrants and collect disaggregated data on malaria and population movements must, therefore, be strengthened.

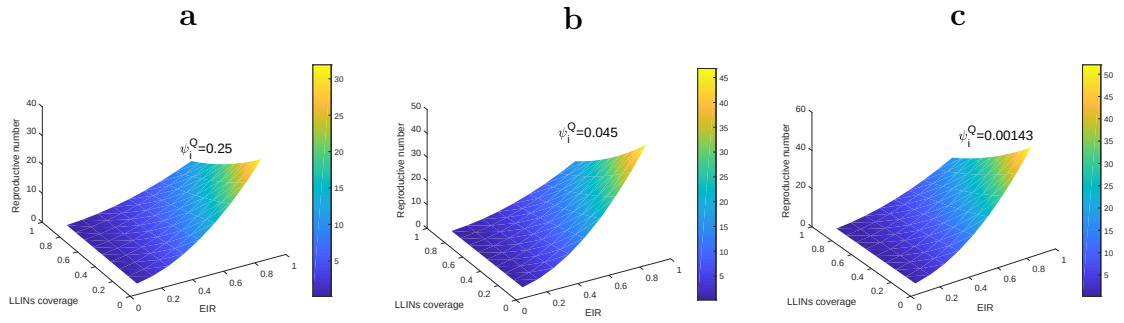

Figure 9: Basic reproduction number and mosquito bitting rate against LLINs Coverage with various migration rate

Table 4: Summaries of expected malaria cases in thousands for the year 2021

		(a)			**(b)**		
	without LLINs		coverage		75% LLINs	coverage	
	Patches	mean	95CI-	95%CI+	mean	95%CI-	95%CI+
Less Mobility	CES	82.4961	61.3250	103.6673	21.9561	13.2877	30.6245
	WBGZ	68.3529	50.1935	86.5124	34.7679	22.8655	46.0030
	WRP	44.4699	31.1922	57.7475	3.5465	0.5448	6.5482
High mobiity	CES	92.5283	69.2978	115.7589	24.2979	15.13518	33.4606
	WBGZ	74.3085	54.7829	93.8341	52.0955	37.0842	67.1069
	WRP	61.7781	44.8534	78.7029	5.7164	0.4322	11.0007

Acknowledgments: The authors wish to thank Robert Snow for the valuable advice provided at the early stages of this work. They are also grateful to Thomas Ujjiga for availing the data used in this research. Abdulaziz Y.A. Mukhtar acknowledges the support of the DSI-NRF Centre of Excellence of Mathematical and Statistical Sciences (CoE-MaSS) towards this research. Rachid Ouifki acknowledges the support of the DSI-NRF SARChI Chair M3B2 grant 82770. Opinions expressed and conclusions arrived at, are those of the authors and are not necessarily to be attributed to the CoE-MaSS or the SARChI Chair M3B2 grant.

Supporting information

S1 Dataset. Weekly malaria cases data

S2 Appendix. Data fitting code

References

[1] M. A. Acevedo, O. Prosper, K. Lopiano, N. Ruktanonchai, T. T. Caughlin, M. Martcheva, C. W. Osenberg and D. L. Smith. Spatial Heterogeneity, Host Movement and Mosquito-Borne Disease Transmission. *PLoS ONE*, **10(6)** (2015) e0127552. doi:10.1371/journal.pone.0127552

[2] L. J. Allen. An introduction to stochastic epidemic models-Part I. *Summer School on Mathematical Modeling of Infectious Disease*,**15** (2008) 1-11.

[3] D. Alonso, M. J. Bouma and M. Pascual. Epidemic malaria and warmer temperatures in recent decades in an East African highland. *The Royal Society*, (2010) doi:10.1098/rspb.2010.2020.

[4] L. Arnold. *Stochastic, Differential Equations: Theory and Applications*, Wiley, New York, 1972

[5] A. Camacho, S. Funk. FitR: Tool box for fitting dynamic infectious disease models to time series. (2017) Version 0.1 Available from: https://github.com/sbfnk/fitR.

[6] C. Chiyaka, J. M. Tchuenche, W. Garira, S. Dube. A mathematical analysis of the effects of control strategies on the transmission dynamics of malaria. *Applied Mathematics and Computation*, **195** (2008); 641-662.

[7] W. E. Collins and G. M. Jeffery. A retrospective examination of sporozoiteand trophozoite-induced infections with *Plasmodium falciparum*: Development of parasitologic and clinical immunity during primary infection. *The American Journal of Tropical Medicine and Hygiene* , 61 (1999); 4–19.

[8] C. Cosner. Models for the effects of host movement in vector-borne disease systems. *Mathematical Biosciences*, **270** (2015); 192-197.

[9] C. Cosner, J. C. Beier, R. S. Cantrell , D. Impoinvi, L. Kapitanskil, M. D. Potts, A. Troyoe, and S. Ruan. The effects of human movement on the persistence of vector-borne diseases. *Journal of Theoretical Biology*, **258** (2009); 550-560.

[10] M. Craig, D. Le Sueur, and B. Snow. A climate-based distribution model of malaria transmission in sub-Saharan Africa. *Parasitology Today*, **15** (1999); 105-111.

[11] D. E. Eyles and M. D. Young. The duration of untreated or inadequately treated *Plasmodium falciparum* infections in the human host. *National Malaria Society*, **10** (1951); 327-336.

[12] J.A.N. Filipe, E.M. Riley, C.J. Drakeley, C.J. Sutherland, A.C. Ghani. Determination of the processes driving the acquisition of immunity to malaria using a mathematical transmission model. *PLOS Computational Biology*, **3** (2007); 2569-2579.

[13] F. Forouzannia, A.B. Gume. Mathematical analysis of an age-structured model for malaria transmission dynamics. *Mathematical Biosciences*, **247** (2014); 80-94.

[14] D. Gao and S. Ruan. A multipach malaria model with logistic growth populations. *SIAM Journal of Applied Mathematics*, **72(3)** (2012); 819-841.

[15] M. Gayer, D. Legros, P. Formenty, M. A. Connolly. Conflict and emerging infectious diseases. *Emerging Infectious Diseases*, **13(11)** (2007) 1625-1631.

[16] D. T. Gillespie. Stochastic Simulation of Chemical Kinetics. *Annu. Rev. Phys. Chem*, **58** (2007) 35–55.

[17] G. Gonzalez Parra, A. J. Arenas and M. R. Cogollo. Positivity and Boundedness of Solutions for a Stochastic Seasonal Epidemiological Model for Respiratory Syncytial Virus (RSV). *Ingeniería y Ciencia*, **13** (2017); 95-121.

[18] J. T. Griffin, N. M. Ferguson and A. C. Ghani . Estimates of the changing age-burden of *Plasmodium falciparum* malaria disease in sub-Saharan Africa. *Nat. Commun*, (2014) 5:3136 doi: 10.1038/ncomms4136.

[19] G. R. Hosack, P. A. Rossignol, P. van den Driessche. The control of vector-borne disease epidemics. *J. Theoret. Biol*, **255** (2008); 16-25.

[20] N. Ingemar. Stochastic models of some endemic infections. *Mathematical Biosciences*, **179** (2002) 1–19.

[21] S. Kim, A. Tridane and D. E. Chang. Human migrations and mosquito-borne diseases in Africa. *Mathematical Population Studies*, **23** (2016); 123-146.

[22] P. V. Le, P. Kumar, M. O. Ruiz. Stochastic lattice-based modelling of malaria dynamics. *Malaria journal*, **17** (2018); https://doi.org/10.1186/s12936-018-2397.

[23] G. Macdonald. The analysis of infection rates in diseases in which super infection occurs. *Tropical Disease Bulletin*, **47** (1950); 907-915.

[24] S. Mandal, R. R. Sarkar, S. Sinha. Mathematical models of malaria-a review. *Malaria Journal*, **10** (2011); https://doi.org/10.1186/1475-2875-10-202.

[25] X. Mao, G. Marion, E. Renshaw. Environmental Brownian noise suppresses explosions in population dynamics. *Stochastic Processes and Their Applications*, **97** (2002); 95-110.

[26] P. Martens and L. Hall. Malaria on the move: Human population movement and malaria transmission. *Emerging Infectious Diseases*, **6(2)** (2000); 103-109.

[27] A. Y. A. Mukhtar, H. B. Munyakazi, R. Ouifki. Assessing the role of climate factors on malaria transmission dynamics in South Sudan. *Mathematical Bioscince*, **310** (2019); 13-23.

[28] A. Y. A. Mukhtar, J. B. Munyakazi, R. Ouifki, A. E. Clark. Modelling the effect of bednet coverage on malaria transmission in South Sudan. *PLoS ONE*, **13(6)** (2018): e0198280. https://doi.org/10.1371/journal.pone.0198280

[29] J. Nedelman. Introductory review: Some new thoughts about some old malaria models. *Math. Biosci*, **73** (1985); 159-182.

[30] G. A. Ngwa W. S. Shu. A mathematical model for endemic malaria with variable human and mosquito populations. *Mathematical and Computer Modelling*, **32** (2000); 747-763.

[31] L. C. Okell, M. Cairns, J. T. Griffin„ et. al. Contrasting benefits of different artemisinin combination therapies as first-line malaria treatments using model-based cost-effectiveness analysis. *Nature communications*, **5** (2014); 5606.

[32] S. Portugsl, H. Drakesmith and M. M Mota. Superinfetion in Malaria, *Plasmodium* shows its iron will. *EMBO reports*, **12** 12(2011): 1233–1242.

[33] S. P. Silal, F. Little, K. I Barnes, L. J. White. Hitting a moving target: a model for malaria elimination in the presence of population movement. *PLoS ONE*, **10(12)** (2015): e0144990. https://doi.org/10.1371/journal.pone.0144990.

[34] SSCCSE: South Sudan counts: Tables from the 5th Sudan population and housing census, 2008. Juba: Government of Southern Sudan: Southern Sudan Centre for Census: Statistics and Evaluation; 2010.

[35] T. Stoddard, A. C. Morrison, G. M. Vazquez-Prokopec. The role of human movement in the transmission of vector-borne pathogens. *PLoS Neglected Tropical Diseases*, **3(7)** (2009): e481.

[36] L. Sattenspiel and K. Dietz. A structured epidemic model incorporating geographic mobility among regions. *Math Biosci*, **128** (1995); 71-91.

[37] R. Ross. The prevention of malaria, volume 2. Murray, London, 1911.

[38] Van den Driessche, P., and Watmough, J. Reproduction numbers and subthreshold endemic equilibria for compartmental models of disease transmission. *Mathematical Bioscience*, **180** (2002); 29-48.

[39] D. I. Wallace, B. S. Southworth, X. Shi, J. W. Chipman, J. W. Githeko. A comparison of five malaria transmission models: benchmark tests and implications for disease control. textitMalaria Journal, **13** (2014). https://doi.org/10.1186/1475-2875-13-268.

[40] D. Wanduku, G.S. Ladde. Fundamental Properties of a Two-scale Network stochastic human epidemic Dynamic model. *Neural, Parallel, and Scientific Computations* **19** (2011); 229-270.

[41] A. Wesolowski, N. Eagle, A. J. Tatem, D. L. Smith, A. M. Noor, R. W. Snow, and C. O. Buckee. Quantifying the impact of human mobility on malaria.*Science*, **338** (2012); 267-270.

[42] WHO. World Malaria Report 2016.

[43] J. Yu, D. Jiang, N. Shi. Global stability of two-group SIR model with random perturbation. *Journal of Mathematical Analysis and Applications*, **360** (2009); 235-244.